E. coli MEP Synthase: Steady-State Kinetic Analysis and Substrate Binding†

Andrew T. Koppisch,‡ David T. Fox,§ Brian S. J. Blagg, and C. D. Poulter*

Department of Chemistry, University of Utah, Salt Lake City, Utah 84112

Received September 20, 2001

ABSTRACT: 2-C-Methyl-D-erythritol-4-phosphate synthase (MEP synthase) catalyzes the rearrangement/reduction of 1-D-deoxyxylulose-5-phosphate (DXP) to methylerythritol-4-phosphate (MEP) as the first pathway-specific reaction in the MEP biosynthetic pathway to isoprenoids. Recombinant *E. coli* MEP was purified by chromatography on DE-52 and phenyl-Sepharose, and its steady-state kinetic constants were determined: $k_{cat} = 116 \pm 8\ s^{-1}$, $K_M^{DXP} = 115 \pm 25\ \mu M$, and $K_M^{NADPH} = 0.5 \pm 0.2\ \mu M$. The rearrangement/reduction is reversible; $K_{eq} = 45 \pm 6$ for DXP and MEP at 150 μM NADPH. The mechanism for substrate binding was examined using fosmidomycin and dihydro-NADPH as dead-end inhibitors. Dihydro-NADPH gave a competitive pattern against NADPH and a noncompetitive pattern against DXP. Fosmidomycin was an uncompetitive inhibitor against NADPH and gave a pattern representative of slow, tight-binding competitive inhibition against DXP. These results are consistent with an ordered mechanism where NADPH binds before DXP.

Isoprenoid compounds represent one of the largest and most diverse groups of natural products, with over 30 000 identified members to date (*1*). These molecules perform a variety of important tasks in their host organisms, including serving as hormones in mammals, antioxidants in plants, and electron carriers during cellular respiration (*2*). Isopentenyl diphosphate (IPP)[1] and dimethylallyl diphosphate (DMAPP) are the five-carbon building blocks used to construct more complicated isoprenoid structures. Until recently, IPP and DMAPP were thought to originate only from acetate via the mevalonate pathway (*3*). However, studies by Rohmer (*4*) and Arigoni (*5*) uncovered an alternate pathway that operates in plants, algae, and bacteria (*6*) where IPP and DMAPP are derived from pyruvate and glyceraldehyde-3-phosphate (see Scheme 1). The two three-carbon precursors are joined in a thiamine diphosphate-mediated condensation catalyzed by 1-deoxy-D-xylulose-5-phosphate (DXP) synthase to give DXP (*7*). DXP is then rearranged and reduced by 2-C-methyl-D-erythritol-4-phosphate synthase (MEP synthase) (also called DXP reductoisomerase or DXP isomeroreductase) to form MEP. DXP has been identified as an intermediate in the synthesis of vitamin B_6 (*8*) and is a likely intermediate in the biosynthesis of B_1 (*9*). Thus, MEP is the first intermediate committed to IPP formation, and the name "methylerythritol phosphate pathway" has recently been suggested for this route (4th European Symposium on Plant Isoprenoids, Barcelona, 1999). MEP is converted to 2-C-methyl-D-erythritol-2,4-cyclodiphosphate by the action of three successive enzymes (*10*−*15*). The remaining steps in the MEP pathway have not been determined.

Scheme 1 : Methylerythritol Phosphate Pathway

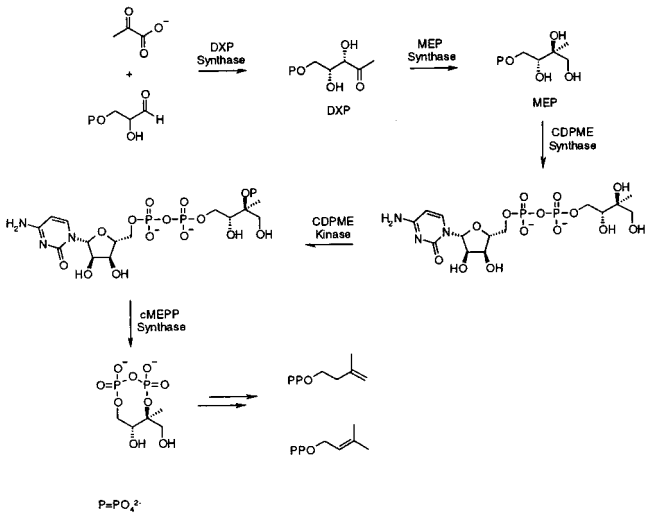

Cloning and overexpression of *E. coli* MEP synthase were reported by Seto and co-workers. The recombinant enzyme was a tetramer of 165 kDa (*16*) and catalyzed the conversion of DXP to MEP in the presence of NADPH and a divalent cation. They proposed that Co^{2+} is the biologically relevant metal on the basis of steady-state kinetic studies, although Mn^{2+} and Mg^{2+} were only slightly less effective. MEP synthases have now been cloned from *Z. mobilis*, *E. coli*, *Mentha x piperita*, *A. thaliana*, *Synechocystis sp.*, *S. coeli-*

† This research was supported by NIH Grant GM 25521.

* To whom correspondence should be addressed. Phone: (801) 581-6685. Fax: (801) 581-4391. E-mail: poulter@chemistry.chem.utah.edu.

‡ American Heart Association, Western States Affiliate Predoctoral Fellow.

§ NIH Biological Chemistry Predoctoral Trainee.

[1] Abbreviations: βME, 2-mercaptoethanol; BSA, bovine serum albumin; DXP, 1-D-deoxyxylulose-5-phosphate; EDTA, ethylenediaminetetraacetic acid; EGTA, ethylene glycol bis(β-aminoethyl ether)-*N*,*N*,*N*′,*N*′-tetraacetic acid; IPP, isopentenyl diphosphate; IPTG, isopropyl-β-D-thiogalactopyranoside; MEP, 2-C-methyl-D-erythritol-4-phosphate; $NADP^+$, nicotinamide adenine dinucleotide phosphate (oxidized form); NADPH, nicotinamide adenine dinucleotide phosphate (reduced form); $NADPH_3$, dihydronicotinamide adenine dinucleotide phosphate; NMR, nuclear magnetic resonance; PMSF, phenylmethylsulfonyl fluoride; Tris, tris(hydroxymethyl)aminomethane; U, unit(s).

10.1021/bi0118207 CCC: $22.00
Published on Web 12/07/2001

Scheme 2 : Reactions Catalyzed by MEP Synthase (A) and Ketol−Acid Reductoisomerase (B)

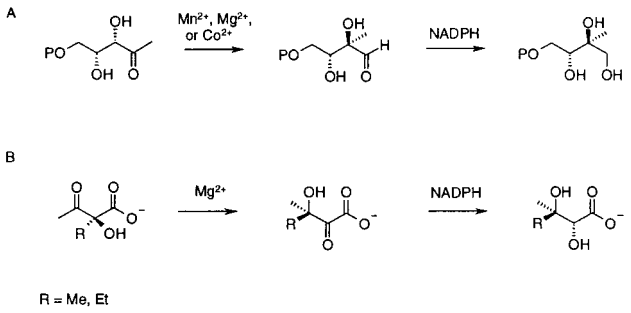

color, and *P. aeruginosa* (*17*−*23*). Several catalytically important conserved amino acids have been identified by site-directed mutagenesis (*24*). Although MEP synthase catalyzes the first dedicated step in the MEP pathway, several reports suggest that synthesis of DXP is the rate-limiting step in isoprenoid formation (*25*−*28*).

The rearrangement catalyzed by MEP synthase is similar to those catalyzed by 3,4-dihydroxy-2-butanone-4-phosphate synthase (*29*) and ketol−acid reductoisomerase (*30*−*33*). Both MEP synthase and the ketol−acid reductoisomerase catalyze NADPH-dependent reductions (see Scheme 2), although a rearranged intermediate analogous to the one found during the ketol−acid reductoisomerase reaction has not been detected for MEP synthase. Additionally, the reactions catalyzed by ketol−acid reductoisomerase are reversible. Although the two reactions mediated by MEP synthase and ketol−acid reductoisomerase are similar, the enzymes do not have similar amino acid sequences.

The MEP pathway is absent in mammals and is considered an attractive target for the development of antibiotics. The enzyme is strongly inhibited by the antibiotic fosmidomycin, and mice infected with the malaria parasite *Plasmodium vinckei* have shown to fully recover upon treatment with this inhibitor (*34*). Seto and co-workers reported that fosmidomycin showed mixed inhibition with a K_i of 38 nM for *E. coli* MEP synthase (*35*), whereas Grolle et al. reported fosmidomycin was competitive with DXP with $K_i = 600$ nM for the *Z. mobilis* enzyme (*17*).

The interest in MEP synthase as a potential target for drug development led us to more fully characterize the enzyme. We now describe experiments which demonstrate that MEP synthase catalyzes a reversible rearrangement/reduction of DXP and MEP by an ordered sequential mechanism and that fosmidomycin is a slow, tight-binding inhibitor.

EXPERIMENTAL PROCEDURES

Materials and General Methods. All reagents were purchased from Aldrich unless otherwise noted. Tris buffers are reported at their observed pH at room temperature (25 °C). $NADPH_3$ was synthesized by the method of Dave et al. (*36*), and fosmidomycin was synthesized using the method reported by Hashimoto et al. (*37*). Protein concentrations were measured using the method of Bradford (*38*). DXP and MEP were synthesized with methods previously reported by this laboratory (*39*, *40*). All nucleotide stock solutions were made fresh daily. NADPH solutions were made in water or D_2O, and the concentration was calculated using $\epsilon^o_{340} = 6.22$ cm^{-1} mM^{-1}. $NADP^+$ stock solutions were made fresh each day in water or D_2O from preweighed ampules of nucleotide (Sigma), and their concentrations were verified by UV spectroscopy using $\epsilon^o_{259} = 18$ cm^{-1} mM^{-1}. $NADPH_3$ stock solutions were made in water, and the concentration was calculated using $\epsilon^o_{290} = 13.75$ cm^{-1} mM^{-1}. Stock solutions of fosmidomycin were made by weighing. Stock solutions of DXP or MEP were prepared in water or D_2O, and their concentrations were determined by the method of Rane and Calvo (*41*). Briefly, an assay was performed using an excess of nucleotide (approximately 5−10-fold higher with DXP, or 900−1000-fold higher with MEP) and a fixed amount of substrate. In each case, the concentration of nucleotide must be sufficient to effectively consume all of the phosphosugar substrate as the equilibrium is reestablished. The amount of nucleotide consumed was determined from the difference of the initial and final absorbance at 340 nm. Concentrations represent the average of 3−4 repetitions. All enzymatic reactions were UV-monitored by changes at 340 nm in 10 mm quartz cuvettes. Nuclear magnetic resonance spectra were acquired at 500 MHz. DNA sequencing was performed at the University of Utah Core Sequencing Facility.

Cloning, Overexpression, and Purification. The gene encoding MEP synthase was amplified from *E. coli* genomic DNA (Sigma) using Klentaq DNA polymerase (Clonetech) and 20 cycles of the following temperatures: denaturation, 94 °C, 75 s; annealing, 48 °C, 2 min; extension, 72 °C, 2 min. The sense primer SBAMDXR (5′-CGCGGATCCAGGAGGTATACATATGAAGCAACTCACCATTCTGGGC-3′) was designed to incorporate an *Nde*I restriction site as well as a *Bam*HI restriction site at the 5′ terminus, while the antisense primer APSTDXR (5′-AAAACTGCAGTCATCAGCTTGCGAGACGCATCACC-3′) was designed to incorporate a *Pst*I site at the 3′ end. Product from the PCR reaction was ligated into the pGEM-T Easy vector (Promega), verified through sequencing, and subsequently subcloned into pHN1+ (*42*) to form pATKII-13763.

E. coli XA-90 (*42*) cells were transformed with pATKII-13763. Cultures of the transformants grown in LB media containing ampicillin (0.1 mg/mL) were induced by the addition of IPTG to a final concentration of 2 μM at an OD of 0.6 and grown for an additional 4 h at 37 °C before being harvested (15 000 rpm, 15 min). A typical 500 mL culture produced roughly 1.8 g of cell paste. Cells were lysed on ice via sonication (3 rounds of 30 s, with a 1 min rest period) in buffer containing 100 mM Tris, pH 7.6, 0.1 mM EDTA, 0.1 mM EGTA, 10 mM BME, 10 μg/mL pepstatin, and 1 mM PMSF. After centrifugation (14 000 rpm, 15 min), the supernatant was passed through a 0.45 nm syringe filter and applied to a DE52 column (2.5 × 30 cm), which had been preequilibrated with 200 mL of buffer A (10 mM potassium phosphate, pH 7.6/10 mM βME). After a further washing with 40 mL of buffer A, the enzyme was eluted from the column using a 440 mL linear gradient (100 to 0% buffer A) with buffer B (300 mM potassium phosphate, pH 7.6/10 mM βME), followed by a 40 mL washing with buffer B. Fractions containing MEP synthase were pooled, concentrated, and mixed 1:1 (v/v) with buffer C (100 mM Tris, pH 7.6/1.5 M ammonium sulfate/10 mM βME). The supernatant was then applied to a phenyl-Sepharose column (2.5 × 35 cm), which had been preequilibrated with 200 mL of buffer D (50 mM Tris, pH 7.6/0.75 M ammonium sulfate/10 mM βME). The column was washed with 90 mL of buffer D

Scheme 3 : Mechanism for Slow, Tight-Binding Inhibition

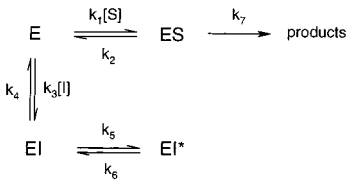

and eluted with a 300 mL linear gradient (100 to 0%) of buffer D to buffer E (50 mM Tris, pH 7.6/10 mM βME) followed by 90 mL of buffer E. Recombinant MEP synthase, >95% pure, was then flash-frozen in 30% glycerol and stored at −80 °C until used.

Initial Velocity Assays for MEP Synthase. Activity for MEP synthase was monitored by the change in absorbance at 340 nm as the nucleotide cofactor was oxidized (assays with DXP) or reduced (assays with MEP). All assay buffers were degassed prior to use. Standard assays were performed at 37 °C with a total volume of either 200 or 400 μL, and contained 100 mM Tris, pH 7.6, 1 mM (Co^{2+} or Mn^{2+}) or 2 mM divalent cation (Mg^{2+}), 1 mg/mL BSA, 0.15 mM nucleotide, and varying concentrations of DXP or MEP. The reactions were initiated by the addition of enzyme. Serial dilutions of enzyme were made into 100 mM Tris buffer, pH 7.0, containing 1 mg/mL BSA. Typically, assays contained 2 nM enzyme. We found the addition of BSA to the reaction buffer was necessary in order to maintain linearity when the enzyme was present at low concentrations. Assays to determine Michaelis−Menten constants were performed in triplicate at 6−7 different concentrations of the variable substrate. Kinetic data were fitted to the standard Michaelis−Menten equations (*43*) using Grafit (Erithacus software) or Kaleidagraph (Synergy software).

Measurement of the Equilibrium Constant by Nuclear Magnetic Resonance Spectroscopy. The equilibrium constant between DXP/NADPH and MEP/$NADP^+$ was measured in D_2O by nuclear magnetic resonance (NMR) spectroscopy. The samples were prepared in D_2O (100%, Aldrich) buffer and contained all of the standard assay components except BSA. Enzyme was dialyzed into D_2O containing buffer prior to use, and the typical enzyme concentration in these assays was 2 μM. At high enzyme concentrations, MEP synthase retained >90% of its original activity for up to 90 min at 37 °C without added BSA. The initial and final nucleotide concentrations were determined by A_{340}, while the molar ratios of MEP and DXP were measured from the relative intensities of the resonances for the methyl group in each compound using the hydroxymethyl resonances of the Tris buffer as an internal standard. The equilibrium constant was calculated using eq 1.

$$K_{eq} = \frac{[NADP^+][MEP]}{[NADPH][DXP]} \quad (1)$$

Equilibrium constants measured at low cofactor concentrations using a NADPH regenerating system were performed as described above with the following adjustments: [$NADP^+$] was reduced to 0.01 mM, the initial [MEP] was 1 mM, and the buffer contained 2.2 mM acetone-d_6 as well as 5 U of *T. brockii* alcohol dehydrogenase (Sigma). The reactions were initiated by addition of 2 μM MEP synthase that had been previously dialyzed into D_2O buffer. Spectra were taken at 30 min intervals for 2 h.

Inhibition Studies. The UV assay described above was used with minor modifications. Initial velocities were measured for four different concentrations of variable substrate at four different concentrations of inhibitor along with the fixed substrate. Initial velocities and concentrations were fit to the equations for competitive (eq 2), noncompetitive (eq 3), or uncompetitive (eq 4) inhibition (*43*):

$$v = \frac{V_{max}[S]}{[S] + K_m\left(1 + \frac{[I]}{K_i}\right)} \quad (2)$$

$$v = \frac{V_{max}[S]}{[S]\left(1 + \frac{[I]}{K_i}\right) + K_m\left(1 + \frac{[I]}{K_i}\right)} \quad (3)$$

$$v = \frac{V_{max}[S]}{[S]\left(1 + \frac{[I]}{K_i}\right) + K_m} \quad (4)$$

to ascertain which pattern was followed.

Preliminary experiments with fosmidomycin suggested that the compound was a slow, tight-binding inhibitor (Scheme 3). Our data are consistent with a mechanism where the inhibitor binds rapidly (represented by EI) with an inhibition constant, K_i, followed by a time-dependent conversion to a more tightly bound state (represented by EI*) with a second inhibition constant, K_i*. We estimated the inhibition constants in two ways. Initially, the reactions were initiated by the addition of enzyme into buffer containing DXP and NADPH. The progress curves were fit to eq 5:

$$\text{absorbance} = v_s t + (v_o - v_s)(1 - e^{-kt})/k \quad (5)$$

which describes the time-dependent conversion of the initial velocity (v_o) to a final velocity (v_s), where k is the observed rate constant for the interconversion of the velocities. An estimate of k was obtained from a series of curves obtained at different inhibitor concentrations. Values for k were also determined by extrapolation as described by Morrison and Walsh (*44*). These values were subsequently used to determine the velocities by fitting the progress curves at different substrate concentrations to eq 5. A standard v vs [I] analysis provided estimates of K_i (using v_o) and K_i* (using v_s). A second estimate for K_i* was obtained directly from reactions that had been preincubated with fosmidomycin. In this case, enzyme, inhibitor, and NADPH were preincubated in buffer at 37 °C for 5 min prior to initiation of the reaction with DXP. One obstacle to this type of analysis is that by preincubating the inhibitor with enzyme, it is possible to saturate the substrate binding sites with inhibitor. Since the binding and release of the inhibitor is slow relative to the time-scale of the assay, this phenomenon results in a "lag phase" in the trace, which is eventually overcome as the K_i* equilibrium is established. We found that 5 min was sufficient to establish full initial binding of fosmidomycin (as determined by the absence of curvature in the trace) without saturating the enzyme with inhibitor. Thus, the final velocity (v_s) was estimated from the linear progress curves,

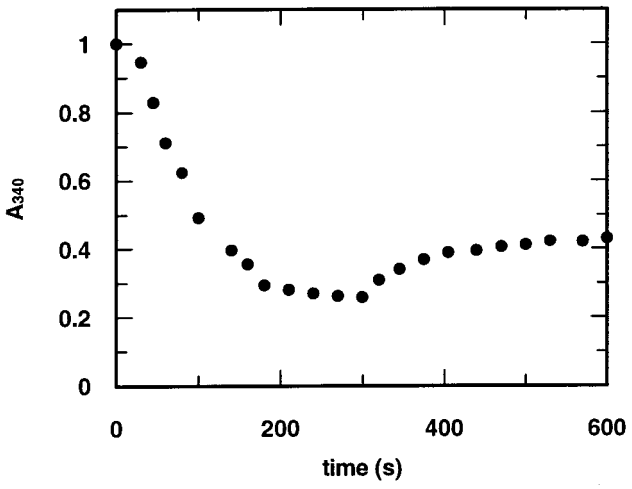

FIGURE 1: Time course for incubation of 0.12 mM DXP and 0.15 mM NADPH with MEP synthase. After 500 s, 0.36 mM $NADP^+$ was added to the sample. The general reaction conditions are described under Experimental Procedures.

and the estimate of K_i* was in good agreement with the value determined from the nonlinear curves. The forward (k_5) and reverse (k_6) rate constants for the interconversion to the tight-binding state EI* were calculated from eqs 6 and 7 (*45*, *46*):

$$k_6 = \frac{k v_s}{v_o} \tag{6}$$

$$K_i^* = K_i\left(\frac{k_6}{k_5 + k_6}\right) \tag{7}$$

RESULTS

MEP Synthase Catalyzes a Reversible Reaction. Although the reactions catalyzed by several ketol−acid reductoisomerases are reversible (*32*, *33*), similar behavior has not previously been reported for MEP synthase. When the enzyme was incubated under conditions where the concentrations of DXP and NADPH were approximately equal, the absorbance at 340 nm decreased as the dihydronicotinamide moiety was oxidized. When no further decrease in absorbance was observed, an excess of $NADP^+$ was added to the sample. As seen in Figure 1, the absorbance increased with time as NADPH was regenerated from $NADP^+$, presumably as MEP was oxidized. When MEP synthase was incubated with $NADP^+$ and a synthetic sample of MEP, an increase in the absorbance at 340 nm was observed with concomitant conversion of MEP to DXP.

The rearrangement/reduction of DXP to MEP presumably occurs in two steps—isomerization of DXP to methylerythrose phosphate, followed by reduction of the aldehyde to give MEP. DXP was the only oxidation product formed from MEP, as determined by ^1H NMR spectroscopy. The methyl resonances of MEP and DXP are well-resolved, sensitive signatures for those two molecules, and the expected chemical shift of the resonance for the aldehyde (or aldehyde hydrate) proton in methylerythrose should be well-resolved from resonances in MEP or DXP. Interfering resonances from NADPH and $NADP^+$ were minimized by initiating the incubation of MEP using only 0.01 equiv of $NADP^+$, a 15-fold reduction over standard assay conditions, and an alcohol dehydrogenase to regenerate $NADP^+$ as the oxidation of MEP proceeded (*46*). The results are summarized in Figure 2. Figure 2a shows the region of the spectrum containing the methyl resonances of MEP and DXP. As the reaction proceeded, the intensity of the methyl resonance in MEP decreased concomitantly with an increase in the intensity in the methyl resonance in DXP. During this time, no resonances were detectable in the region where aldehyde and aldehyde hydrate protons resonate, even at a high spectrum amplitude (Figure 2b). Thus, we estimate that methylerythrose phosphate constitutes no more than 0.2% of the sum of MEP and DXP. Attempts to trap methylerythrose phosphate with sodium borohydride or *N*-methylnitrosohydrazine were unsuccessful.

Several observations suggest that our inability to detect methylerythrose phosphate is not an artifact of our experiments. Although some alcohol dehydrogenases reduce a wide range of ketones and aldehydes (*47*), we think it is unlikely that the *T. brockii* enzyme we used to regenerate $NADP^+$ selectively reduced methylerythrose phosphate to MEP in the presence of DXP and a large excess of acetone. Even if methylerythrose phosphate composed 10% of the equilibrium mixture [a number that is several orders of magnitude greater than reported for ketol−acid reductoisomerases (*33*) and at least 5-fold greater than our limits of detection], acetone would still be present in a 22-fold molar excess. In addition, erythrose-4-phosphate, a commercially available analogue for methylerythrose phosphate that lacks the C-2 methyl group, is a poor substrate for the dehydrogenase, with a K_m at least 100-fold higher than acetone. In a control experiment, we found that MEP synthase oxidizes NADPH in the presence of erythrose phosphate, albeit at a slower rate than DXP.[2] Although we could not detect methylerythrose phosphate, our experiments do not exclude the aldehyde as an intermediate. Calvo and co-workers also found that 3-hydroxy-3-methyl-2-oxobutyrate, the intermediate they observed in the ketol−acid reductoisomerase reaction, did not accumulate to an appreciable extent (*33*).

MEP Synthase Utilizes Mg^{2+}, Mn^{2+}, or Co^{2+} as a Divalent Metal. Contrary to previous reports (*16*, *17*, *24*), we found that Co^{2+}, Mn^{2+}, and Mg^{2+} were equally effective as required divalent cations when the reactions were carried out in buffer containing BSA. Optimal concentrations were 1 mM for Mn^{2+} and Co^{2+}, and 2 mM for Mg^{2+}at pH ~7.5−8.0. Table 1 lists the kinetic parameters obtained from a standard Michaelis−Menten analysis. The equilibrium constant for the reaction $K_{eq} = 45 \pm 6$ was measured with DXP or MEP as the starting substrate.

The K_m^{DXP} value reported here for the *E. coli* MEP synthase is similar to those previously reported for the *Z. mobilus* ($K_m^{DXP} = 300\ \mu M$) (*17*) and *S. coelicolor* ($K_m^{DXP} = 190\ \mu M$) (*22*) enzymes, as well as previously published parameters for the *E. coli* enzyme ($K_m^{DXP} = 99\ \mu M$) (*24*). Although there is some variation in the reported K_m values for NADPH, none differ by more than an order of magnitude. We believe that differences between our values for k_{cat} and those reported previously for the *E. coli* enzyme are due to

[2] Erythrose phosphate from Sigma is 60−75% pure. The major impurity is glyceraldehyde 3-phosphate. Incubations of MEP synthase with glyceraldehyde 3-phosphate and NADPH did not generate $NADP^+$ under the conditions of our experiment.

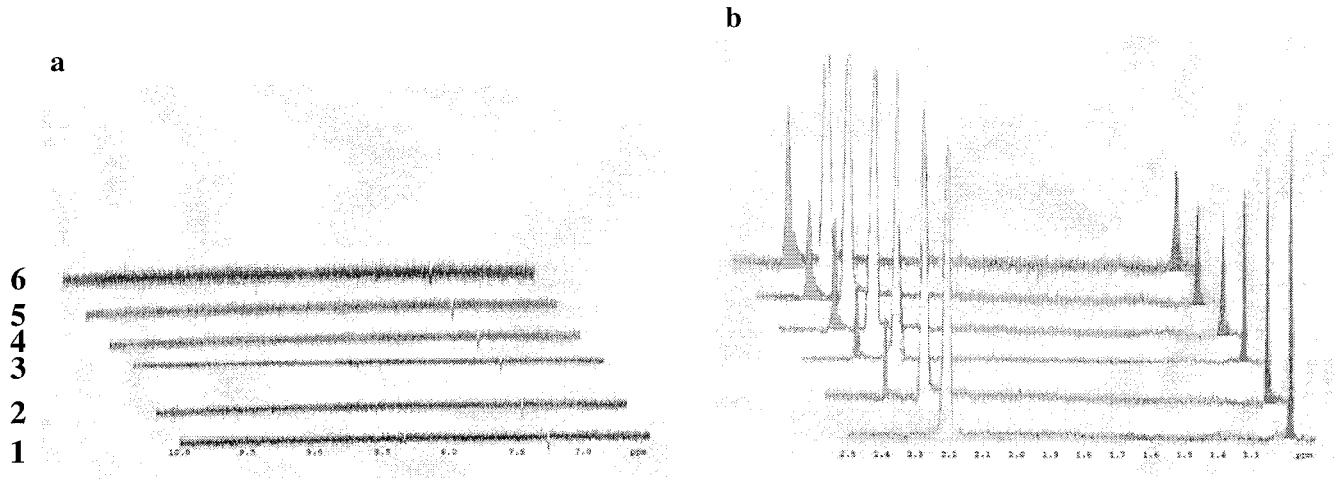

FIGURE 2: Analysis of the time course for incubation of 1 mM MEP and 0.15 mM $NADP^+$ by ^1H NMR spectroscopy. Reactions were performed in thick-walled NMR tubes as described under Experimental Procedures and were initiated by addition of the enzyme. The region of the spectra which contains resonances for the methyl groups in MEP (1.18 ppm) and DXP (2.32 ppm) is shown, as well as the region where resonances for aldehyde or aldehyde hydrate should appear at (1) 0 min, (2) 20 min, (3) 30 min, (4) 60 min, (5) 90 min, and (6) 90 min with a sample of synthetic DXP (0.1 μmol) added externally. The resonance at 2.20 ppm is from residual nondeuterated acetone.

Table 1: Steady-State Kinetic Constants for MEP Synthase in the Presence of Mn^{2+}, Mg^{2+}, and Co^{2+}

substrate	$K_m(Mn^{2+})$ (μM)	$K_m(Mg^{2+})$ (μM)	$K_m(Co^{2+})$ (μM)	$k_{cat}(Mn^{2+})$ (s^{-1})	$k_{cat}(Mg^{2+})$ (s^{-1})	$k_{cat}(Co^{2+})$ (s^{-1})
DXP	175 ± 45	115 ± 25	12 ± 2	107 ± 8	116 ± 8	50 ± 4
MEP	390 ± 120	330 ± 100	20 ± 5	61 ± 6	50 ± 8	4 ± 1
NADPH[a]	1 ± 0.4	0.5 ± 0.2	0.8 ± 0.2	–	–	
$NADP^+$	30 ± 6	25 ± 3	10 ± 2	–	–	

[a] The concentrations of NADPH used to determine these parameters approach the detection limit of our assay.

Scheme 4: Structures of Fosmidomycin and $NADPH_3$

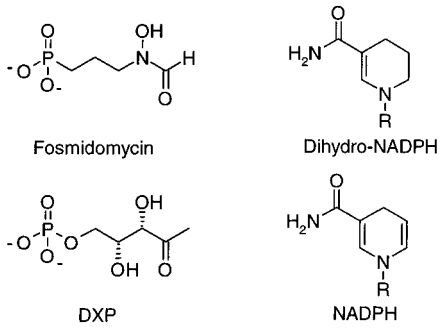

instability of the protein at low concentrations. Cane and co-workers have recently reported $k_{cat} = 22\ s^{-1}$ for the *E. coli* enzyme at 25 °C (*22*). This is in good agreement with our value, given that our assays were conducted closer to the optimum temperature for the enzyme (50 °C) (*24*).

Addition of Substrates Is Ordered. Fosmidomycin and $NADPH_3$ were used as dead-end inhibitors for DXP and NADPH, respectively, to distinguish between random and ordered binding mechanisms for MEP synthase (Scheme 4). $NADPH_3$ is an unreactive analogue of NADPH that is easy to prepare (*36*, *48*), and fosmidomycin is thought to inhibit MEP synthase by mimicking methylerythrose phosphate. Double reciprocal plots of initial velocities versus [DXP] and [NADPH] at fixed concentrations of $NADPH_3$ are shown in Figure 3. $NADPH_3$ was a competitive inhibitor when NADPH was the varied substrate, and gave a noncompetitive pattern against DXP.

The progress curves obtained with fosmidomycin had a marked curvature at higher concentrations of the inhibitor. As seen in Figure 4a, the rate of the reaction decreased rapidly during the first 2 min from an initial velocity (v_o) at short reaction times to a final value (v_s). This type of behavior is typical for a slow binding inhibitor (*44*). When the enzyme was preincubated in buffer containing fosmidomycin and NADPH for 5 min before the reaction was initiated by adding DXP, the progress curves were linear, and the rates were similar to those measured for samples without preincubation (Figure 4b). Progress curves were nonlinear, like those in Figure 4a, when MEP synthase was preincubated with only fosmidomycin or NADPH. These results suggest that binding is ordered and NADPH adds before the inhibitor.

Double reciprocal plots for inhibition by fosmidomycin at varied concentrations of DXP and NADPH are shown in Figure 5. Fosmidomycin gave an uncompetitive profile when NADPH was varied (Figure 5a) and either a competitive (Figure 5b) or a noncompetitive (Figure 5c) profile with respect to DXP depending upon whether v_o or v_s was analyzed. This phenomenon is typical of many slow, tight-binding competitive inhibitors where the noncompetitive profile is an artifact of the sluggish K_i* binding equilibrium. The rates for interconversion between the initial and final binding states, $k_5 = 3.0 \pm 0.46\ min^{-1}$ and $k_6 = 0.33 \pm 0.05\ min^{-1}$, were determined from eqs 6 and 7, respectively. The relevant parameters are listed in Table 2.

DISCUSSION

Concerns about the emergence of new bacterial strains that are resistant to the current generation of antibiotics have stimulated the search for new drugs (*49*). The methyl-erythritol phosphate (MEP) pathway has emerged as an attractive target. Mutations in genes that block biosynthesis of isopentenyl diphosphate and dimethylallyl diphosphate

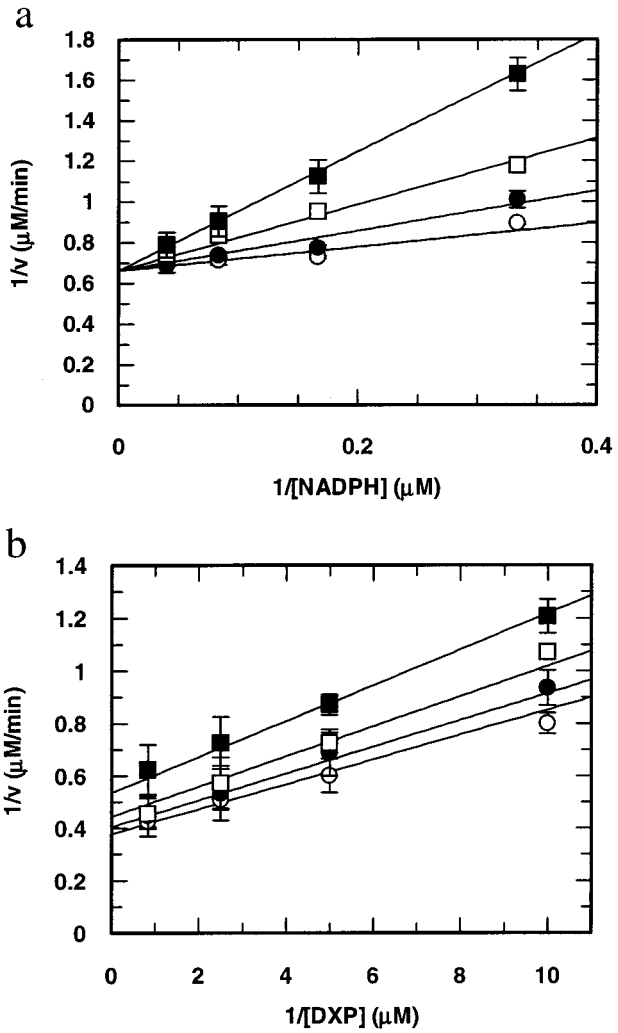

FIGURE 3: Double reciprocal plots for inhibition by $NADPH_3$. (a) Initial velocity vs [NADPH] at 2 (○), 5 (●), 10 (□), and 20 μM (■) $NADPH_3$ and 0.15 mM DXP. (b) Initial velocity vs [DXP] at 2 (○), 5 (●), 10 (□), and 20 μM (■) $NADPH_3$ and 10 μM NADPH.

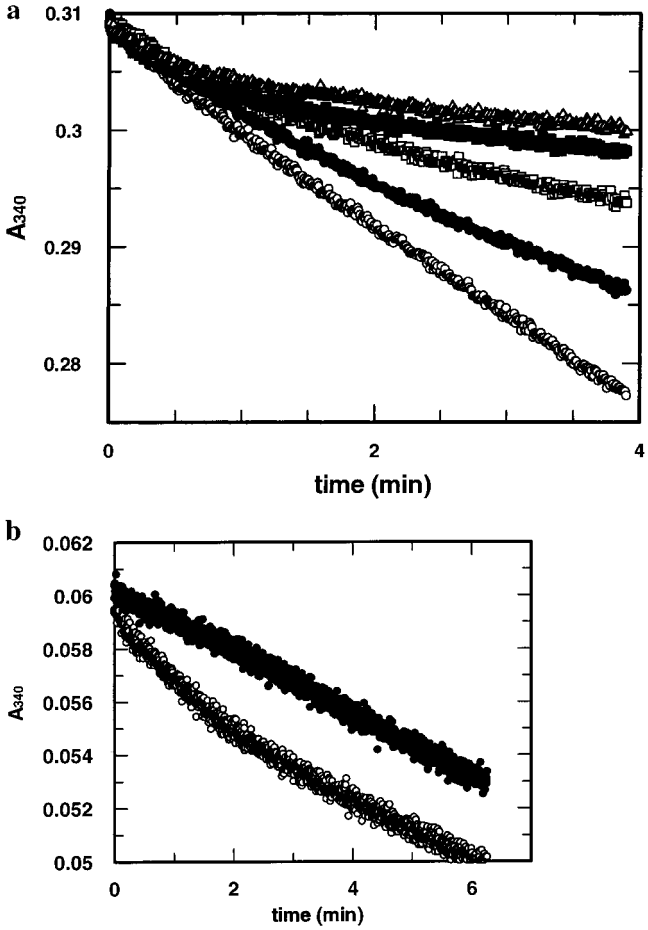

FIGURE 4: Progress curves for synthesis of MEP. (a) 0 (○), 50 (●), 100 (□), 200 (■), and 250 nM (△) fosmidomycin, no preincubation. (b) 100 nM fosmidomycin, no preincubation (○) and after a 5 min preincubation of enzyme with fosmidomycin and NADPH (●).

from DXP in bacteria are lethal. These two building blocks are synthesized in humans via the mevalonate (MVA) pathway. Thus, the early steps in isoprenoid biosynthesis in humans are orthogonal to those in many pathogenic bacteria, providing an opportunity to develop inhibitors against enzymes in the MEP pathway that selectively block isoprenoid biosynthesis in many bacteria without affecting their human hosts.

Methylerythritol phosphate synthase catalyzes the first pathway-specific reaction in the MEP pathway. The synthesis of MEP from DXP proceeds in two steps—a [1.2] shift to generate methylerythrose phosphate followed by reduction of the aldehyde to give MEP. These reactions are similar to the rearrangement/reductions catalyzed by ketol−acid reductoisomerases. DXP, like acetolactate or 2-acetohydroxybutyrate, exists in equilibrium with the isomerized/reduced products, and for both classes of reductoisomerases, the equilibrium concentrations of rearranged intermediates are low. Interestingly, there is no significant similarity between the amino acid sequences of the two enzymes.

Seto and co-workers originally reported that *E. coli* MEP synthase (*16*) prefers Mn^{2+}, but concluded more recently that Co^{2+} is the physiologically relevant metal on the basis of k_{cat}/K_m measurements (*24*). In contrast, we found that Mg^{2+}, Mn^{2+}, and Co^{2+} were essentially equally effective as cofactors for recombinant *E. coli* MEP synthase in incubations where BSA was included in the buffer. The catalytic efficiencies of the enzyme (k_{cat}/K_m) were similar, and a lower k_{cat} for Co^{2+} was offset by a lower K_m^{DXP}. Since cellular concentrations of Mg^{2+} are much higher than Co^{2+} or Mn^{2+}, we conclude that Mg^{2+} is the normal cofactor in vivo.

A kinetic analysis based on dead-end inhibitors for DXP and NADPH indicated that the addition of substrates to MEP synthase is strictly ordered, with DXP adding before NADPH. Ordered mechanisms were also reported for *E. coli* (*33*), *S. typhimurium* (*31*), and spinach ketol−acid reductoisomerase, where NADPH binds before acetolactate (*32*). We selected fosmidomycin as a competitive inhibitor for DXP based on reports for *Z. mobilus* MEP synthase. However, we found that fosmidomycin was not a classical competitive inhibitor against DXP, but instead displayed slow, tight-binding behavior. For example, the double reciprocal plot of initial velocity versus [DXP] at different fixed concentrations of fosmidomycin was noncompetitive at the concentrations of DXP examined (*44*). Similar profiles have been reported for several other cases of slow, tight-binding inhibition (*50, 51*). We investigated several different combinations of fosmidomycin, MEP, and NADPH in preincubation experiments with MEP synthase to determine what conditions were necessary to facilitate binding of the

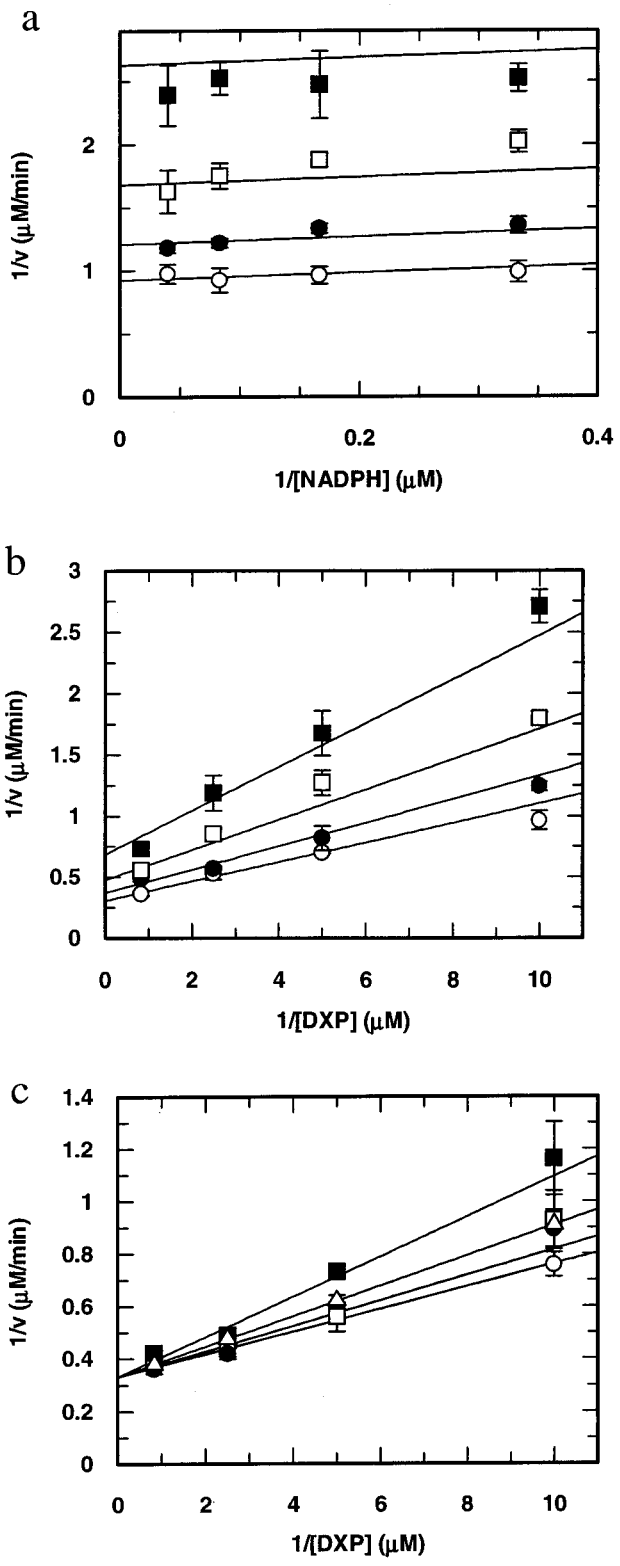

FIGURE 5: Double reciprocal plots for inhibition by fosmidomycin. (a) Initial velocity versus [NADPH] at 10 (○), 25 (●), 50 (□), and 100 nM (■) fosmidomycin and 0.15 mM DXP. (b) Initial velocity versus [DXP] at 10 (○), 25 (●), 50 (□), and 100 nM fosmidomycin (■) and 10 μM NADPH. (c) Initial velocity versus [DXP] at 20 (○), 50 (●), 100 (□), and 200 nM (■) fosmidomycin and 10 μM NADPH, without preincubation.

inhibitor. The slow, tight-binding behavior of fosmidomycin was eliminated only when DXP synthase was preincubated with the inhibitor and NADPH, and the reaction was then initiated by addition of DXP. This observation suggests a mandatory ordered sequence where NADPH binds before fosmidomycin. Similar behavior has been documented for other slow, tight-binding inhibitors (*44*, *51*), including *N*-hydroxy-*N*-isopropyloxamate, a slow, tight-binding inhibitor of *E. coli* ketol−acid reductoisomerase (*52*).

Table 2: Inhibition Constants and Observed Inhibition Patterns for MEP Synthase with Fosmidomycin and $NADPH_3$

inhibitor	substrate	pattern	K_i (nM)
$NADPH_3$	NADPH	competitive	3000
$NADPH_3$	DXP	noncompetitive	41000
fosmidomycin[a]	DXP	noncompetitive	21
fosmidomycin[a]	NADPH	uncompetitive	40
fosmidomycin[b]	DXP	competitive	215
fosmidomycin[b]	NADPH	uncompetitive	1070

[a] K_i and inhibition patterns determined from v_s. The double reciprocal pattern for DXP appears noncompetitive; it is better represented by an equation describing slow, tight-binding competitive inhibition (see Discussion). [b] K_i and inhibition patterns determined from v_o.

The slow, tight-binding properties of fosmidomycin explain differences between our results with *E. coli* MEP synthase and other studies with the *E. coli* enzyme and MEP synthase from other sources. Seto and co-workers reported $K_i = 38$ nM for the fosmidomycin and a mixed inhibition pattern with *E. coli* MEP synthase (*35*). Grolle et al. reported that fosmidomycin was competitive against DXP with $K_i = 600$ nM for the *Z. mobilis* enzyme (*17*). We could duplicate either result depending on whether the double reciprocal plots were constructed from v_o (a competitive profile, $K_i = 215$ nM, corresponding to K_i) or v_s (a noncompetitive profile, $K_i = 21$ nM, corresponding to K_i*). The existence of two distinguishable K_i values for slow, tight-binding inhibitors is believed to reflect an initial binding step, followed by isomerization of the enzyme to a state which binds the inhibitor more tightly ($K_i^* < K_i$).

Several reports have suggested that synthesis of DXP is the rate-limiting step in isoprenoid biosynthesis by the MEP pathway (*25*−*28*). This proposal was primarily based on an increase in the amount of isoprenoid biosynthesis in cells where DXP synthase was overexpressed as compared with overexpression of MEP synthase. Our results are consistent with another explanation. Overexpression of DXP synthase should result in an increase in the cellular concentration of DXP. Since the decarboxylation of pyruvate during condensation with glyceraldehyde-3-phosphate is irreversible, the size of the pool of DXP available for MEP synthase should increase once MEP synthase and the branch point enzymes in thiamine and pyridoxine biosynthesis are saturated, provided there is a supply of pyruvate and glyceraldehyde phosphate. In contrast, the isomerization/reduction catalyzed by MEP synthase is reversible. When the branch point enzymes that use MEP are saturated, the size of the pool is determined by the concentrations of the substrates and products of MEP synthase. It is also possible that the flux of metabolites moving through the pathway in wild-type cells is controlled at the translational level. Additional work will be needed to resolve these issues.

ACKNOWLEDGMENT

We thank Dr. C. M. Harris for helpful discussions.

REFERENCES

1. Poulter, C. D., and Rilling, H. C. (1981) in *Biosynthesis of Isoprenoid Compounds* (Porter, J. W., and Spurgeon, S. L., Eds.) Vol. 1, pp 161−224, Wiley, New York.
2. Sacchetini, J. C., and Poulter, C. D. (1997) *Science 277*, 1788−1790.
3. Bochar, D. A., Freisen, J. A., Stauffacher, C. V., and Rodwell, V. W. (1999) in *Comprehensive Natural Products Chemistry* (Barton, D., and Nakanishi, K., Eds.) Vol. 2, pp 15−44, Elsevier, Oxford.
4. Flesch, G., and Rohmer, M. (1988) *Eur. J. Biochem. 175*, 405−411.
5. Arigoni, D., Sagner, S., Latzel, C., Eisenreich, W., Bacher, A., and Zenk, M. H. (1997) *Proc. Natl. Acad. Sci. U.S.A. 94*, 10600−10605.
6. Eisenreich, W., Schwarz, M., Cartayrade, A., Arigoni, D., Zenk, M. H., and Bacher, A. (1998) *Chem. Biol. 5*, R221−R233.
7. Lois, L. M., Campos, N., Putra, S. R., Danielsen, K., Rohmer, M., and Boronat, A. (1998) *Proc. Natl. Acad. Sci. U.S.A. 95*, 2105−2110.
8. Begley, T. P. (1996) *Nat. Prod. Rep. 13*, 177−185.
9. Cane, D. E., Du, S., Robinson, K., Hsiung, Y., and Spenser, I. D. (1999) *J. Am. Chem. Soc. 121*, 7722−7723.
10. Rohdich, F., Wungsintaweekul, J., Fellermeier, M., Sagner, S., Herz, S., Kis, K., Eisenreich, W., Bacher, A., and Zenk, M. H. (1999) *Proc. Natl. Acad. Sci. U.S.A. 96*, 11758−11763.
11. Kuzuyama, T., Takagi, M., Kaneda, K., Dairi, T., and Seto, H. (2000) *Tetrahedron Lett. 41*, 703−706.
12. Luttgen, H., Rohdich, F., Herz, S., Wungsintaweekul, J., Hecht, S., Schuhr, C. A., Fellermeier, M., Sagner, S., Zenk, M. H., Bacher, A., and Eisenreich, W. (2000) *Proc. Natl. Acad. Sci. U.S.A. 97*, 1062−1067.
13. Kuzuyama, T., Takagi, M., Kaneda, K., Watanabe, H., Dairi, T., and Seto, H. (2000) *Tetrahedron Lett. 41*, 2925−2928.
14. Herz, S., Wungsintaweekul, J., Schuhr, C. A., Hecht, S., Luttgen, H., Sagner, S., Fellermeier, M., Eisenreich, W., Zenk, M. H., Bacher, A., and Rohdich, F. (2000) *Proc. Natl. Acad. Sci. U.S.A. 97*, 2426−2490.
15. Takagi, M., Kuzuyama, T., Kaneda, K., Watanabe, H., Dairi, T., and Seto, H. (2000) *Tetrahedron Lett. 41*, 3395−3398.
16. Takahashi, S., Kuzuyama, T., Watanabe, H., and Seto, H. (1998) *Proc. Natl. Acad. Sci. U.S.A. 95*, 9879−9884.
17. Grolle, S., Bringer-Meyer, S., and Sahm, H. (2000) *FEMS Microbiol. Lett. 191*, 131−137.
18. Kuzuyama, T., Takahashi, S., Watanabe, H., and Seto, H. (1998) *Tetrahedron Lett. 39*, 4509−4512.
19. Lange, B. M., and Croteau, R. (1999) *Arch. Biochem. Biophys. 365*, 170−174.
20. Schwender, J., Muller, C., Zeidler, J., and Lichtenthaler, H. K. (1999) *FEBS Lett. 455*, 140−144.
21. Proteau, P. J., Woo, Y. H., Williamson, T., and Phaosiri, C. (1999) *Org. Lett. 1*, 921−923.
22. Cane, D. E., Chow, C., Lillo, A., and Kang, I. (2001) *Bioorg. Med. Chem. 9*, 1467−1477.
23. Altincicek, B., Hintz, M., Sanderbrand, S., Wiesner, J., Beck, E., and Jomaa, H. (2000) *FEMS Microbiol. Lett. 190*, 329−333.
24. Kuzuyama, T., Takahashi, S., Takagi, M., and Seto, H. (2000) *J. Biol. Chem. 275*, 19928−19932.
25. Kuzuyama, T., Takagi, M., Takahashi, S., and Seto, H. (2000) *J. Bacteriol. 182*, 891−897.
26. Miller, B., Heuser, T., and Zimmer, W. (2000) *FEBS Lett. 481*, 221−226.
27. Harker, M., and Bramley, P. M. (1999) *FEBS Lett. 448*, 115−119.
28. Estevez, J. M., Cantero, A., Reindl, A., Reichler, S., and Leon, P. (2001) *J. Biol. Chem. 276*, 22901−22909.
29. Gotze, E., Kis, K., Eisenreich, W., Yamauchi, N., Kakinuma, K., and Bacher, A. (1998) *J. Org. Chem. 63*, 6456−6457.
30. Arfin, S. M., and Umbarger, H. E. (1969) *J. Biol. Chem. 244*, 1118−1127.
31. Shematek, E. M., Arfin, S. M., and Diven, W. F. (1973) *Arch. Biochem. Biophys. 158*, 132−138.
32. Dumas, R., Job, D., Ortholand, J. Y., Emeric, G., Greiner, A., and Douce, R. (1992) *Biochem. J. 288*, 865−874.
33. Chunduru, S. K., Mrachko, G. T., and Calvo, K. C. (1989) *Biochemistry 28*, 486−493.
34. Jomaa, H., Wiesner, J., Sanderbrand, S., Altincicek, B., Weidemeyer, C., Hintz, M., Turbachova, I., Eberl, M., Zeidler, J., Lichtenthaler, H. K., Soldati, D., and Beck, E. (1999) *Science 285*, 1573−1576.
35. Kuzuyama, T., Shimizu, T., Takahashi, S., and Seto, H. (1998) *Tetrahedron Lett. 39*, 7913−7916.
36. Dave, K. G., Dunlap, R. B., Jain, M. K., Cordes, E. H., and Wenkert, E. (1968) *J. Biol. Chem. 243*, 1073−1074.
37. Hashimoto, M., Hemmi, K., Kamiya, T., and Takeno, H. (1980) U.S. Patent 819, 554.
38. Bradford, M. M. (1976) *Anal. Biochem. 72*, 248−254.
39. Blagg, B. S. J., and Poulter, C. D. (1999) *J. Org. Chem. 64*, 1508−1511.
40. Koppisch, A. T., Blagg, B. S. J., and Poulter, C. D. (2000) *Org. Lett. 2*, 215−217.
41. Rane, M. J., and Calvo, K. C. (1997) *Arch. Biochem. Biophys. 338*, 83−89.
42. Myers, L. C., Terranova, M. P., Nash, H. W., Markus, M. A., and Verdine, G. L. (1992) *Biochemistry 31*, 4541−4547.
43. Segel, I. H. (1985) *Enzyme Kinetics: Behavior and Analysis of Rapid Equilibrium and Steady-State Enzyme Systems*, pp 18−224, Wiley, New York.
44. Morrison, J. F., and Walsh, C. T. (1989) *Adv. Enzymol. 61*, 201−301.
45. Williams, J., and Morrison, J. (1979) *Methods Enzymol. 63*, 437.
46. Copeland, R. A. (2000) *Enzymes*, 2nd ed., pp 188−265, Wiley, New York.
47. Lamed, R. J., and Zeikus, J. G. (1981) *Biochem. J. 195*, 183−190.
48. Jarstfer, M. B., Blagg, B. S. J., Rogers, D. H., and Poulter, C. D. (1996) *J. Am. Chem. Soc. 118*, 13089−13090.
49. Davies, J. (1994) *Science 264*, 375−382.
50. Templeton, M. D., Sullivan, P., and Shepherd, M. G. (1984) *Biochem. J. 224*, 379−388.
51. Williams, J. W., Morrison, J. F., and Duggleby, R. G. (1979) *Biochemistry 18*, 2567−2573.
52. Aulabaugh, A., and Schloss, J. V. (1990) *Biochemistry 29*, 2824−2830.

BI0118207